Optics Letters

1D speckle-learned structured light recognition

Purnesh Singh Badavath,[1] Venugopal Raskatla,[1,2] and Vijay Kumar[1,*]

[1]Department of Physics, National Institute of Technology Warangal, Telangana, 506004, India
[2]Current address: Optoelectronics Research Centre and Centre for Photonic Metamaterials, University of Southampton, Highfield, Southampton, SO17 1BJ, UK
*vijay@nitw.ac.in

Received 1 December 2023; revised 25 December 2023; accepted 15 January 2024; posted 22 January 2024; published 13 February 2024

In this Letter, we introduce a novel, to the best of our knowledge, structured light recognition technique based on the 1D speckle information to reduce the computational cost. Compared to the 2D speckle-based recognition [J. Opt. Soc. Am. A 39, 759 (2022)], the proposed 1D speckle-based method utilizes only a 1D array (1×n pixels) of the structured light speckle pattern image ($n \times n$ pixels). This drastically reduces the computational cost, since the required data is reduced by a factor of 1/n. A custom-designed 1D convolutional neural network (1D-CNN) with only 2.4 k learnable parameters is trained and tested on 1D structured light speckle arrays for fast and accurate recognition. A comparative study is carried out between 2D speckle-based and 1D speckle-based array recognition techniques comparing the data size, training time, and accuracy. For a proof-of-concept for the 1D speckle-based structured light recognition, we have established a 3-bit free-space communication channel by employing structured light-shift keying. The trained 1D CNN has successfully decoded the encoded 3-bit gray image with an accuracy of 94%. Additionally, our technique demonstrates robust performance under noise variation showcasing its deployment in practical cost-effective real-world applications.

https://doi.org/10.1364/OL.514739

In structured light, the intensity and phase of the optical field will be spatially varying. The most commonly known families of structured light are Laguerre–Gaussian (*LG*) beams and Hermite–Gaussian (*HG*) beams. Structured light has garnered considerable significance encompassing fields like telecommunications, quantum topography, optical trapping, and imaging [1,2]. One of the emerging fields of structured light applications is communication [3]. Theoretically, structured light can offer infinite channels in a limited bandwidth by employing its infinite orthogonal basis set [4]. As the mode-division-multiplexing (MDM) is independent of wavelength and polarization multiplexing techniques [5], structured light provides an additional degree of freedom to encode the information in multiple dimensions simultaneously and increase the information exchange capacity in free-space optical communication (FSOC) channels [6,7]. The traditional methods of structured light detection, like interference [7,8] and diffraction [6,9], entail complexity because they require high-quality sensitive optical components and a high degree of alignment for accurate structure light recognition. The complexity of the recognition is reduced by introducing artificial intelligence (AI) models. The AI-based structured light recognition models have increased the detection speed and accuracy, which leads to real-time optical communication [10,11].

Various neural networks (NNs) have been proposed to decode the information encoded in structured light beams from their direct intensity profiles [12,13] or interferograms [14,15] and are being deployed in optical communication links. However, despite improved performance, existing methods face limitations in detection accuracy due to alignment constraints. The necessity to capture the entire beam restricts the number of structured light beams that can be employed. This limitation is attributed to the direct proportionality of mode order to beam size, imposing constraints on the receiver aperture size. Addressing this challenge, a demultiplexing method based on speckle patterns has been proposed [16–20] in fiber and FSO communication. This method allows information decoding from a smaller structure light speckle pattern region with a sufficient number of speckle grains. By relaxing alignment constraints, it enables intensity degenerate structure light recognition [12] and non-line-of-sight optical communication [21,22]. Up to this point, speckle-based demultiplexing techniques have utilized 2D speckle images and 2D neural networks (NNs) for OAM beam recognition. The use of 2D images necessitates 2D-pixel cameras, extensive storage capacity, computationally intensive NNs, increased processing time, and advanced computational resources for effective classification.

To decrease the computational cost/time and increase the economic feasibility while maintaining the fidelity of the structure light demultiplexing, we are reporting a novel 1D far-field speckle-learned recognizing (FSLR) method. In this method, a custom-designed 1D convolutional neural network (CNN) is trained and tested on randomly mapped 1D arrays of the 2D far-field structured light speckle patterns. The 1D speckle arrays have been mapped at a random angle from the captured Laguerre–Gaussian (*LG*) beam's speckle pattern images, which showcases the alignment and rotational independence of the 1D FSLR method. The minimum data requirements are optimized by computing the accuracy and training time as a function of the number of observations per class and the size of the 1D arrays. A comparison of 2D speckle-based recognition and 1D FSLR methods is also carried out to demonstrate the advantage of the 1D FSLR method. For proof of concept, a 3-bit 100 × 100 pixel gray-level image has been sent across an FSOC

channel. The image has been encoded using the structured light-shift keying (SL-SK) method and decoded with 94% accuracy with the 1D FSLR method. Finally, the structured light speckle patterns have been simulated with white Gaussian noise and Kolmogorov turbulence to resemble the real-world background noise. The 1D FSLR method has been performed on simulated noisy speckle patterns, showcasing its robust performance under noisy conditions.

The complex amplitude of the *LG* beams is expressed as

$$LG_{m,l}(r) = A_{l,m}\left(\frac{W_0}{W(z)}\right)\left(\frac{\rho}{W(z)}\right)^{l}\mathcal{L}_m^l\left(\frac{2\rho^2}{W^2(z)}\right)\times e^{-\frac{\rho^2}{W^2(z)}}\times e^{-ikz-ik\frac{\rho^2}{2R(z)}\mp il\phi+i(l+2m+1)\zeta(z)}, \quad (1)$$

where $\mathcal{L}_m^l$, $W(z)$, and $R(z)$ represent the Laguerre polynomial, beam width, and wavefront's radius of curvature, respectively. Integers l and m are azimuthal and radial indices, respectively. The intensity of the speckle fields corresponding to the *LG* beam is given by

$$I_S = [\mathcal{F}\{u(r)e^{i\phi_{R_i}(r)}\}]\times[\mathcal{F}\{u(r)e^{i\phi_{R_i}(r)}\}]^*, \quad (2)$$

where I_S represents the intensity of the simulated speckle field, $u(r)$ represents the complex amplitude of the *LG* beam, ϕ_{R_i} represents the spatially varying random phase across the plane, and $\mathcal{F}$ represents the Fourier transform.

The experimental realization of the 1D FSLR method is shown in Fig. 1(a). The spatial light modulator's (SLM) active area is illuminated with a 3 mW Gaussian laser beam through a beam splitter, and the required vortex phase hologram is updated at the SLM. The required *LG* beam is isolated using an aperture from the diffracted beams of the SLM. The *LG* beam is propagated through the free space and passed through a rotating diffuser placed at the front focal plane of the convex lens of focus f = 12.5cm. The generated far-field speckle pattern is imaged by using a CMOS camera (Thorlabs-CS235CU) at the back focal plane of the convex lens.

Experimentally captured *LG* beams, their speckle patterns, and randomly mapped 1D speckle arrays are shown in Fig. 1(b). We have captured 2000 far-field speckle pattern images per beam for eight *LG* beams ($m = 0$; $l = 1-8$); in total, we have captured 16,000 (2000×8) images. The 1D cross-line arrays have been mapped at a random angle across the captured 2D far-field speckle pattern images. In the 1D FSLR, only 1D speckle arrays are used to classify the *LG* beams with the 1D CNN.

CNNs have performed exceptionally well in OAM classification with multiple degrees of freedom in communication, imaging, data encryption, etc. [23]. Among CNNs, 1D CNNs are specifically designed for processing 1D data such as audio signals, health monitoring, or other types of 1D signals that vary over time. The architecture of the custom-designed 1D CNN consists of a sequential input layer, three sets of 1D convolutional layers, a ReLu layer, and a normalization layer, followed by a 1D global average pooling layer, a fully connected layer, a SoftMax layer, and a classification layer. The numbers of filters and filter sizes of the three 1D convolutional layers are 4, 8, 16 and 5, 10, 15, respectively. The designed 1D CNN is trained by using an Adam optimizer with a constant learning rate of 0.0001 for 200 epochs and has only a maximum of 2.4 k total learnable parameters. The 1D CNN is trained and tested on the 1D arrays extracted from the experimentally captured far-field speckle patterns.

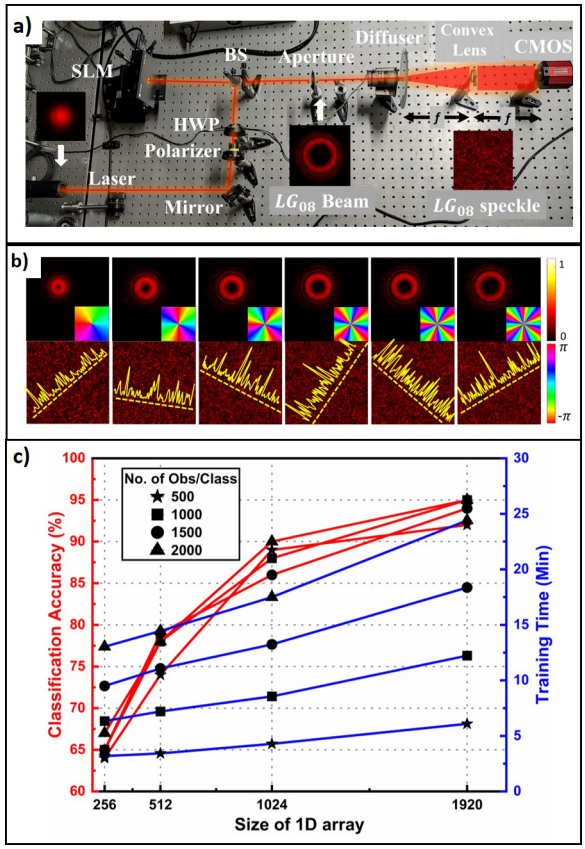

Fig. 1. (a) Experimental setup to generate structured light beams and their speckle patterns. (b) Top row: intensity images of LG_{01-06} beams (left to right). Bottom row: intensity images of the speckle patterns and randomly mapped 1D speckle arrays. (c) Classification accuracy and training time versus the size of the 1D array for different observation samples per class. The results shown are computed on a workstation with a GPU (Nvidia RTX A5000, 24 GB).

The classification accuracy and training time of the 1D CNN will depend on the size of each 1D array and the number of samples (1D arrays) per class (LG beams). The size of the 1D speckle arrays varied from 1×256 to 1×1920 pixels to optimize the classification accuracy and training time. We also varied the number of samples per class from 500 to 2000. The classification accuracies and training time as a function of the size of the 1D array and the number of samples per class are shown in Fig. 1(c). One can conclude that increasing the length of the arrays would significantly increase the classification accuracy rather than increasing the number of samples per class. By trading off the size of the 1D array and the number of samples per class, high classification accuracy can be achieved with minimal data and computational cost.

To demonstrate the importance of the 1D FSLR method over 2D FSLR and to fairly compare the results between the 1D and 2D FSLR, a 2D CNN has been designed analogous to the 1D CNN architecture. The sequential input, 1D convolutional, and 1D global average pooling layers in the 1D CNN are replaced by the image input layer, 2D convolutional layer, and 2D global average pooling layer, respectively. The 2D data has been mapped from the captured speckle patterns as a group of pixels of size $n\times n$ at random places. The 1D data of size $1\times n$ pixels arrays has been mapped at random angles to perform the classification.

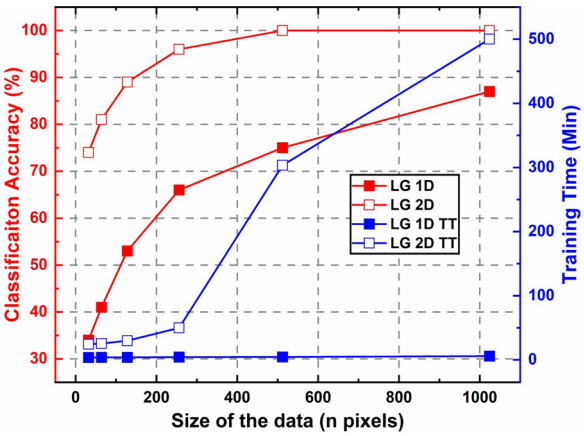

Fig. 2. Size-dependent classification accuracies for experimentally captured 1D arrays (1 × n pixels) and 2D Images (n × n pixels) and their corresponding network training times (TTs). The networks are trained on a workstation with a GPU (Nvidia RTX A5000, 24 GB) with 1000 samples per class.

The classification accuracies and training time of the 2D CNN and 1D CNN at different sizes of the images and arrays have been shown in Fig. 2.

A similar accuracy can be achieved by employing the 1D FSLR in less training time than the 2D FSLR. This effectively shows the superiority of the 1D FSLR method over the 2D FSLR method. The trained 1D CNN with the highest classification accuracy is deployed in a 3-bit SL-SK FSOC channel for a proof of concept of the 1D FSLR method. We have encoded a 3-bit gray-level image in *LG* beams ($m = 0$; $l = 1 - 8$) using the SL-SK encoding scheme. The trained 1D CNN on 1×1920 pixels has successfully reconstructed the image with a 0.056 bit-error rate (BER). The schematic diagram for the experimental realization of the established 3-bit SL-SK FSOC channel using the 1D FSLR method is shown in Fig. 3. To harness the full spectrum of *LG* beams, astigmatic transformed speckle pattern images have been captured by replacing the convex lens with a cylindrical lens ($f = 15cm$) in the experimental setup shown in Fig. 1(a). The 1000 astigmatic transformed speckle pattern images have been captured for each *LG* modes ($m = 0$, $l = \pm 1 - \pm 8$). The 1D CNN trained on the 1D arrays from astigmatic transformed speckle patterns achieved a classification accuracy of 73% by optimizing the data size.

To check the validity and robustness under the real-world noise, in the structured light beams, additive white Gaussian noise (AWGN) has been added to the structured light, and corresponding noisy speckle fields have been simulated. The values of the SNR (in dB) are varied from 0 dB (power of signal = power of noise) to 30 dB to study the effects of AWGN on the *LG* speckle fields and their classification accuracy. The SNR value in AWGN can be calculated using Eq. (3):

$$SNR_{dB} = 10log_{10}\left(\frac{P_s}{P_n}\right), \tag{3}$$

where P_s and P_n are the power of the signal and power noise, respectively. The simulated noisy speckles of LG_{04} with different SNRs are shown in Fig. 4. The 1D CNN is trained on simulated noisy speckle arrays of *LG* beams of size 1×1920 pixels for 1000 samples per class. The achieved accuracies by employing the 1D FSLR method on simulated noisy *LG* beam 1D arrays are given in Table 1. We also trained our model on Kolmogorov turbulence ($C_n^2 = 1.5\text{e-}4m^{-2/3}$) simulating atmospheric turbulence and attained 79% classification accuracy with 1000 samples per class wherein each sample has a length of 1×1920 pixel array.

The 2D CNN performs the convolution, feature learning, and pooling process at the 2D spatial dimension, which is analogous to the parallel computing of the spatial pixels of

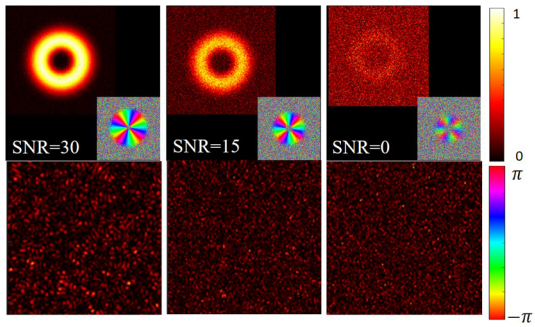

Fig. 4. Simulated AWGN LG_{04} beams and its speckle pattern with different levels of SNR.

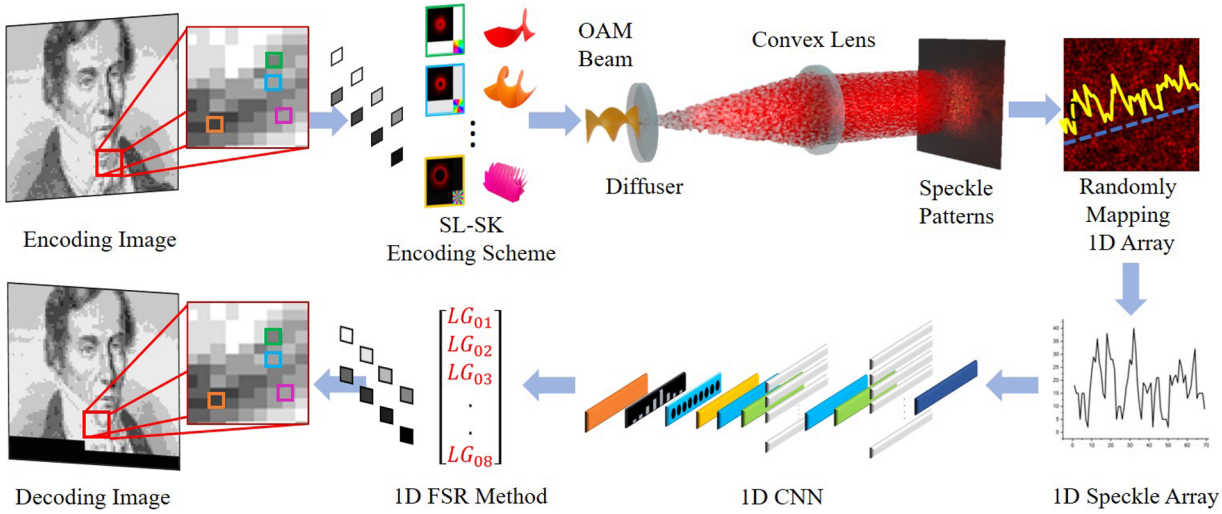

Fig. 3. The schematic diagram for the experimental realization of image encoding using SL-SK and decoding with the 1D FSLR method.

Table 1. Achieved Classification Accuracies by 1D CNN for Different SNR Levels on LG Beams Using the 1D FSLR Method

SNR (dB)	No Noise	30	25	20	15	10	5	0
Accuracy (%)	95	91	88	73	44	18	14	13

captured speckle patterns and needs high-end computational resources. The 1D FSLR uses only $1/n^{th}$ of the data compared to the 2D FSLR, which drastically reduces the computational cost and can increase the training and recognition speed. The 1D FSLR method holds the potential to boost the real-time optical communication speed by employing the structured light's high spectral efficiency and the 1D FSLR's low computational cost and time. The proposed 1D FSLR can be easily deployed in the non-graphical processing unit (GPU) low-end computational resource too. On Intel i7-9700 CPU-32-GB RAM, it takes 3 and 35 min to train the 1D CNN on 1×32 and 1×1024 pixel speckle arrays, respectively with 1000 observations per class.

In conclusion, we have successfully demultiplexed the structured light beams by employing only a 1D far-field speckle array, which consists of less than $1/n^{th}$ of the data employed in traditional AI-based demultiplexing techniques using images of size $n \times n$. This marks a substantial leap in reducing the data by $1/n^{th}$ times thus significantly reducing computational cost and training time and at the same time maintaining fidelity and robustness. A custom design 1D CNN with only 2.4 k learnable parameters is used for faster training and testing, which can be easily supported on low-end computers without GPU. We have also found the minimum data and the number of samples per class required to achieve the optimum classification accuracy by size-dependent classification accuracy study. The designed 1D CNN has achieved a maximum of 98% classification accuracy for 1×1920 pixel length and 2000 observations per class. The trained 1D CNN model has successfully demultiplexed the encoded a 3-bit gray image with a 0.056 BER. This illustrates the high fidelity of the 1D FSLR method in the established SL-SK FSOC channel. Further, the noise-dependent study on various simulated data proves the robustness and reliability of the 1D FSLR in noisy FSOC channels with low computational cost and high feasibility. The proposed 1D FSLR scheme is also applied to the Hermite–Gaussian beam and gives similar results.

The proposed scheme could be a solution for high-capacity information transfer optical communication channels due to reduced training and classification time. The proposed 1D CNN architecture holds promise for future optimization, enabling heightened complexity while preserving network fidelity and simultaneously reducing computational time. This method can be augmented with wavelength and polarization division-multiplexing techniques to increase the data transfer rates. The 1D FSLR method could be a viable solution for the low-power consumption optical communication employing deep learning, which can be deployed in energy-limited applications like ground-to-space, space-to-space, and satellite optical communication.

The 1D speckle-based recognizing scheme could open a new research field to extend it to other wavelength spectrums for increasing the range and avoid atmospheric turbulence and scintillation, which is quite common in the optical domain. Not only limited to communication, but the 1D FSLR method could be used in diverse applications like an alternative way to analyze optical data in metrology, speckle-based bio-imaging, and other relevant applications.

Funding. Science and Engineering Research Board, India (SRG/2021/001375).

Acknowledgment. We acknowledge Prof. Nirmal K. V, University of Hyderabad for allowing us to use the lab facility.

Disclosures. The authors declare no conflicts of interest.

Data availability. Data underlying the results presented in this paper are not publicly available at this time but may be obtained from the authors upon reasonable request.

REFERENCES

1. H. Rubinsztein-Dunlop, A. Forbes, M. V. Berry, *et al.*, J. Opt. **19**, 013001 (2017).
2. Y. Shen, X. Wang, Z. Xie, *et al.*, Light: Sci. Appl. **8**, 90 (2019).
3. A. E. Willner, K. Pang, H. Song, *et al.*, Appl. Phys. Rev. **8**, 041312 (2021).
4. J. Wang, J. Y. Yang, I. M. Fazal, *et al.*, Nat. Photonics **6**, 488 (2012).
5. H. Huang, G. Xie, Y. Yan, *et al.*, Opt. Lett. **39**, 197 (2014).
6. A. Trichili, C. Rosales-Guzmán, A. Dudley, *et al.*, Sci. Rep. **6**, 27674 (2016).
7. Y. Ren, C. Liu, K. Pang, *et al.*, Opt. Lett. **42**, 4881 (2017).
8. P. Ma, X. Liu, Q. Zhang, *et al.*, Opt. Lett. **47**, 6037 (2022).
9. J. M. Hickmann, E. J. S. Fonseca, W. C. Soares, *et al.*, Phys. Rev. Lett. **105**, 053904 (2010).
10. S. Avramov-Zamurovic, J. M. Esposito, and C. Nelson, J. Opt. Soc. Am. A **40**, 64 (2023).
11. B. Li, H. Luan, K. Li, *et al.*, J. Opt. **24**, 094003 (2022).
12. P. L. Neary, J. M. Nichols, A. T. Watnik, *et al.*, J. Opt. Soc. Am. A **38**, 954 (2021).
13. M. Krenn, R. Fickler, M. Fink, *et al.*, New J. Phys. **16**, 113028 (2014).
14. H. Wang, X. Yang, Z. Liu, *et al.*, Nanophotonics **11**, 779 (2022).
15. B. P. da Silva, B. A. D. Marques, R. B. Rodrigues, *et al.*, Phys. Rev. A **103**, 063704 (2021).
16. V. Raskatla, B. P. Singh, S. Patil, *et al.*, J. Opt. Soc. Am. A **39**, 759 (2022).
17. V. Raskatla, P. S. Badavath, and V. Kumar, Opt. Eng. **62**, 036104 (2023).
18. V. Raskatla, P. S. Badavath, and V. Kumar, Opt. Eng. **61**, 063114 (2022).
19. V. Raskatla, P. S. Badavath, V. Kumar, *et al.*, Opt. Photonics News **33**, 51 (2022).
20. Z. Wang, X. Lai, H. Huang, *et al.*, Sci. China Phys. Mech. Astron. **65**, 244211 (2022).
21. P. S. Badavath, V. Raskatla, T. P. Chakravarthy, *et al.*, Appl. Opt. **62**, G53 (2023).
22. P. S. Badavath, V. Raskatla, V. Kumar, *et al.*, Opt. Photonics News **34**(12), 50 (2023).
23. Z. Wan, H. Wang, Q. Liu, *et al.*, ACS Photonics **10**, 2149 (2023).